Applied Physics A (2019) 125:99
https://doi.org/10.1007/s00339-019-2382-6

Applied Physics A
Materials Science & Processing

Boron film laser deposition by ultrashort pulses for use as neutron converter material

Priscila Costa[1] · Marcus P. Raele[1] · Noé G. P. Machado[1] · André F. Silva[1] · Nilson D. Vieira Jr.[1] · Frederico A. Genezini[1] · Ricardo E. Samad[1]

Received: 6 September 2018 / Accepted: 2 January 2019 / Published online: 12 January 2019
© Springer-Verlag GmbH Germany, part of Springer Nature 2019

Abstract

This study investigated the production of boron films by femtosecond pulsed laser deposition (PLD) to be used as converters on bulk semiconductor neutron detectors. The ablation threshold of metallic boron was determined and the film growth was studied as a function of deposition time (5–90 min) and laser pulse energy (35–530 μJ). The films were characterized by scanning electron microscopy (SEM), revealing a flaky morphology, optical profilometry, which determined the films thicknesses (from 80 nm up to 4 μm), Ion Beam Analysis (IBA) that assessed their elemental composition and X-ray diffraction (XRD), which revealed an amorphous structure. In addition, a thermal load study was performed to evaluate the heat flux onto the substrate during deposition process. Stable boron films obtained show that the femtosecond PLD process is reliable and reproducible for the fabrication of thick boron coatings.

1 Introduction

Boron films can be used in a number of technological applications due to their chemical, physical and nuclear properties [1–5], and in optics, for instance, boron films are used as absorption filters in the extreme UV range. One of the main applications of boron films is neutron detection [6–8], in which they are used as a conversion material for semiconductor detectors. By the high cross-sectional nuclear reaction $^{10}B(n,\alpha)^{7}Li$, an incident neutron reacts with boron atoms producing electrically charged particles (α and ^{7}Li particles) that can create a detectable electrical signal. In this application, the film thickness should be optimized to ensure maximum conversion and also minimize self-absorption of the emitted particles [9]. The role of the boron in this field has gained importance mostly due to the ^{3}He crisis [10], which combines high demand with low production of ^{3}He, the most sought neutron converter until now, resulting in soaring prices.

Boron is a nontoxic element, commercially accessible [11], but not readily available as a shelf product in the convenient form of thin sheets [12], probably a result of manufacturing difficulties due to its high melting point [7, 13], along with a low commercial demand. Therefore, in order to achieve a viable and reliable way to produce boron films and compounds, several methods using different techniques were proposed: magnetron sputtering [10], e-beam evaporation [14], chemical vapor deposition (CVD) [15, 16] and pulsed laser deposition (PLD) [7, 17, 18].

PLD has considerable advantages over CVD [14] since it produces films with lower contamination, smaller residual stress, and better adhesion. The CVD technique uses chemically hazardous materials and needs high temperatures, while PLD needs no chemical inputs or target preparation and is a versatile technique due to a relatively simple experimental setup [19]. Boron film deposition was also reported using the e-beam technique [7], which produced coatings that were not stable and did not present good adhesion.

The magnetron sputtering technique is used mainly for industrial applications [20] such as large area coatings, requires a minimum pressure [21] that affects the structure and density of the deposited film. In addition, high temperatures are needed to improve the film adhesion [22].

One of the PLD limitations is related to non-uniformity of the film thickness due to the plume expansion geometry, which, according to the Anisimov model [23], follows an ellipsoid distribution, thus leading to thicker film at the center and thinner at its edges. Nonetheless, when

✉ Priscila Costa
pcosta@ipen.br

[1] Nuclear and Energy Research Institute, IPEN-CNEN/SP, Av. Prof. Lineu Prestes, 2242, Cidade Universitária, São Paulo, SP CEP 05508-000, Brazil

considering areas of a few mm^2, it is possible to assume that the film thickness is uniform. For larger areas is possible to move the substrate away from the target to obtain a more uniform film. With the purpose of neutron conversion, the atomic arrangement (either a crystalline or an amorphous structure) is not important, and the sole critical property is the density of available boron nuclei. Taking into consideration these limitations, PLD is a suitable technique [6] to produce thick, small size, neutron converters.

The literature reports PLD production of pure or compound boron films using mainly excimer [18] or Nd:YAG [13, 24–26] lasers. When using pulses longer than a few nanoseconds [27], as in the case of Nd:YAG and excimer lasers, thermal processes are dominant and the ablation process occurs as a consequence of material heating, melting and evaporation, with further developments depending on the pulse duration, energy and intensity [28–30]. When a melting puddle is formed before evaporation, liquid material can be ejected, resulting in the deposition of clusters and droplets in the substrate [19, 28], creating an inhomogeneous film. This may be an issue when ablating a very high melting point material as boron. It is possible to partially overcome this problem by using excimer lasers, which produce more energetic photons, but are rather bulky and present handling problems with the gases used in the lasing process [28]. On the other hand, Nd:YAG lasers are a mature technology and are commonly used for PLD [28] due to its reliability, low cost, high energy pulses, low beam divergence and low maintenance needs. However, boron films obtained by PLD technique using nanosecond pulses tend to present pronounced rates of target wear, which is not ideal considering the high cost of this material in its pure or isotopically enriched form (aimed at more efficient neutron conversion).

For laser pulses with duration shorter than a few tens of picoseconds, known as ultrashort pulses, the timescales involved change the mechanism of light–matter interaction. The pulse duration is shorter than the time required for the material's ions to vibrate, and only its electrons are heated by direct excitation [27, 31]. After the pulse has finished, those excited electrons rapidly relax their energy to the lattice, quickly rising the material temperature above its boiling point, promoting spallation and/or phase explosion processes [30, 32–35] before significant thermal conduction occurs [28, 30]. Controlling the pulses fluence, the balance of phase explosion and spallation can be adjusted, originating an ablation plume mostly composed of atomized material, increasing the homogeneity of a film deposited on a substrate. Since the light–matter interaction occurs mainly via electron heating, it does not strongly rely on the target material characteristics, only on its type (metal, dielectric, semiconductor) [36], and materials with high thermal conductivity and boiling point can be easily ablated to produce films.

Some studies report boron films grown using femtosecond lasers, but basic data, such as ablation threshold [17] or deposition rate [17, 37], are not always presented, and many details of the methodology adopted are not explained.

Reproducibility and cost are crucial elements when developing reliable devices, so, to achieve this goal, the characteristics of the femtosecond laser–matter interaction are likely to overcome the nanosecond issues. The ablation process, when appropriately controlled, does not eject droplets [30] nor tiny chips that have poor adhesion to the substrate, but an atomized material, resulting in a more efficient and controlled film deposition.

Previous studies by our group showed that, for neutron conversion, films with thicknesses in the range 2.7–3.2 µm [9] are needed. This range was obtained by numerical simulation [9], optimizing the α particles flux from the film considering their self-absorption and the neutron conversion.

The objective of the present work was to study the fs-PLD of boron film dependence on the pulses focusing and energy aiming to produce films with thicknesses in the 2.7–3.2 µm range for use as converters for neutron detection in a silicon photodiode.

2 Materials and methods

The femtosecond pulsed laser system used is a Ti:Sapphire CPA (Femtopower Compact Pro CE-Phase HP/HR from Femtolasers), generating 25 fs (FWHM) pulses centered at 775 nm with 40 nm of bandwidth (FWHM), at 4 kHz repetition rate, and energy per pulse below 800 µJ. The target was a ^{10}B 96% enriched boron disc (diameter: 25.4 mm, thickness: 2 mm) from American Elements.

2.1 Boron ablation threshold fluence determination

Initially, the boron ablation threshold fluence, F_{th}, and its dependence on the pulses superposition, N, were determined using the D-Scan technique [6, 38], and the results are shown in Fig. 1. The ablation threshold dependence on the pulses superposition, $F_{th}(N)$, exhibits the behavior expected of a metal [39], which can be described by:

$$F_{th}(N) = F_{th,1} N^{S-1}, \tag{1}$$

where $F_{th,1} = (0.89 \pm 0.05)$ J/cm^2 is the ablation threshold for a single pulse, and $S = 0.84 \pm 0.01$ is the incubation parameter, both obtained from the fit of Eq. (1) to the experimental data ($\chi^2_{red} = 2.3$).

2.2 Pulsed laser deposition setup

The experimental setup for the boron film deposition (Fig. 2) consists of a motorized kinematic mirror mount that can tilt

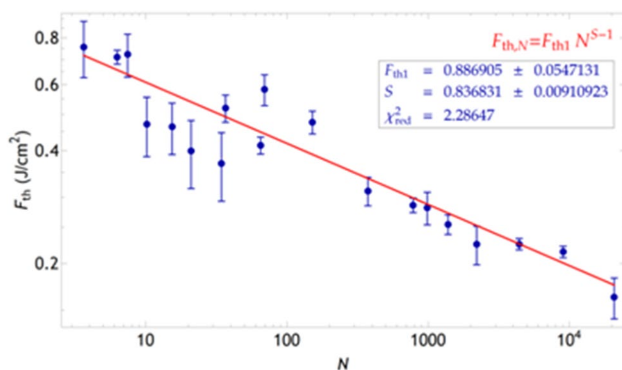

Fig. 1 Boron ablation threshold fluence dependence on the pulse superposition, $F_{th}(N)$ obtained by the D-Scan technique

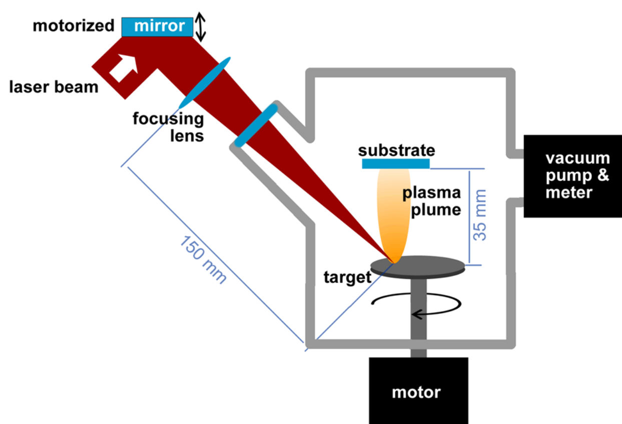

Fig. 2 Experimental setup of boron pulsed laser deposition by femtosecond pulses

the beam to raster its focus over the target surface. After the mirror, a 150 mm focusing lens is positioned close to an optical window of the vacuum chamber, inside which a target is continually rotated by a DC motor (100 rpm). The movement promoted by this motor combined with the raster done by the mirror continuously changes the surface ablated by the laser, ensuring a superposition of about 15 pulses per spot. For this superposition, the ablation threshold value is $F_0 = (0.57 \pm 0.04)$ J/cm^2, calculated from Eq. (1), with the values obtained from the fit. Boron films were deposited on the surface of microscope slides (26×76 mm^{2}substrates), which were positioned 35 mm away from the target. The vacuum is generated by a turbo molecular pump (Pfeiffer HiCube vacuum station), reaching a final pressure of 1×10^{-3} mTorr, which rises to 1×10^{-1} mTorr during the boron ablation.

The 150 mm lens' calculated focal spot radius on the target surface is ~ 15 µm, considering an $M^2 = 1.5$ for the laser beam. This value leads to minimum pulse energy of 4.0 µJ to ablate the boron, considering the $F_0 = 0.57$ J/cm^2

Table 1 Laser pulse energies, fluences (F) and fluence ratio of the ablation threshold (F/F_0)

Pulse energy (µJ)	F (J/cm^2)	F/F_0
37 ± 6	5.2 ± 0.8	9
177 ± 6	25.0 ± 0.8	44
530 ± 7	168.7 ± 1.0	296

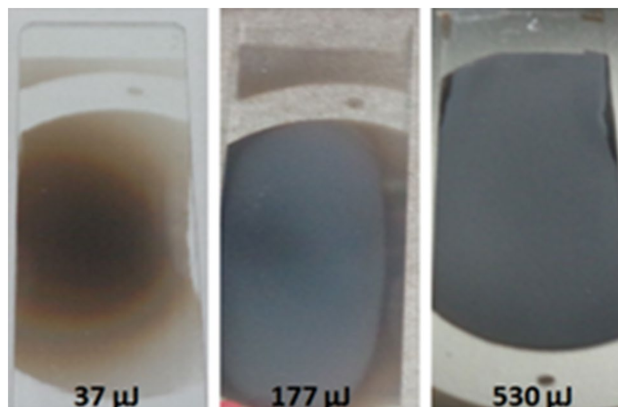

Fig. 3 Boron films deposited during 60 min for different energies, 37, 177 and 530 µJ, over microscope slides

ablation threshold calculated for 15 pulses. Boron thin films were deposited in triplicate, by varying the deposition times between 20 and 90 min, and the pulse conditions are shown in Table 1.

3 Results and discussion

Figure 3 shows boron films deposited for 60 min with the three different pulse energies. The film produced at the lowest energy, 37 µJ, is brown and shows interference rings close to its edge, typical of submicron interference films. On the other hand, the films produced with the higher energies (177 µJ and 530 µJ) are alike, presenting an opaque and grayish aspect, indicating that they are thick enough to absorb the incident light, thus preventing the occurrence of interference rings. This thickness variation among samples is due to the fact that the quantity of ablated material per shot increases with the pulse energy, resulting in a denser boron plume and a higher deposition rate.

To determine the films thicknesses, we used an optical profilometer. This method is reported in literature [13, 37], but those works only present the nominal values, without uncertainties, and no specific detail of the measurement procedure is given.

For this reason, we developed our own methodology to measure the films thicknesses. The method consisted of

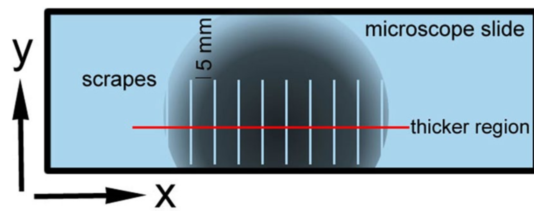

Fig. 4 Methodology used to determine film thickness

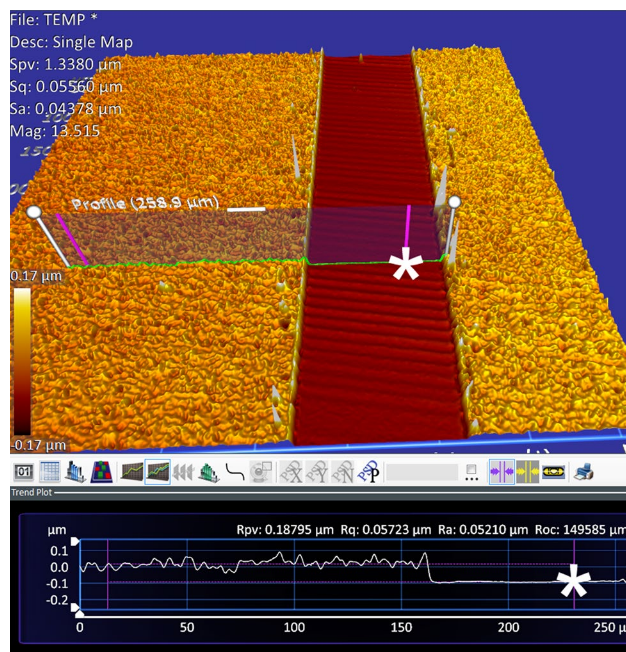

Fig. 5 Optical profilometry of a boron film scrape (*) showing ~0.1 µm thickness

scraping, with a hard metal edge, ten lines spaced 5 mm over the film, taking care to not damage the substrate (Fig. 4), and measuring the film thickness by the optical profilometer (Zygo ZeGage) where it is thicker (about its center, red line on Fig. 4). Figure 5 shows the measurement of one of the scraped lines in which the film thickness can be readily determined.

Figure 6 shows the correlation between thickness and the scraped lines for the 177 µJ pulses, a representative film, and the whole film thickness was taken as the mean (red dashed line) of the eight central measurements (darker points). This thickness variation is due to the ablation plume geometry, and has been already reported in the literature [13]. The final film thickness was the mean value of three repeated laser conditions, for the different laser energies as a function of deposition time is shown in Fig. 7, and a linear trend can be observed.

The growth rate for each pulse energy was obtained from the linear fit of the experimental data presented in

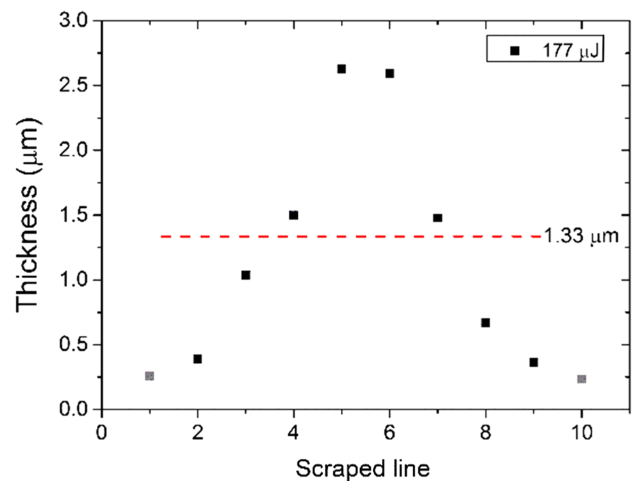

Fig. 6 Scraped lines' thickness. The gray points were not used to calculate the mean (red dashed line)

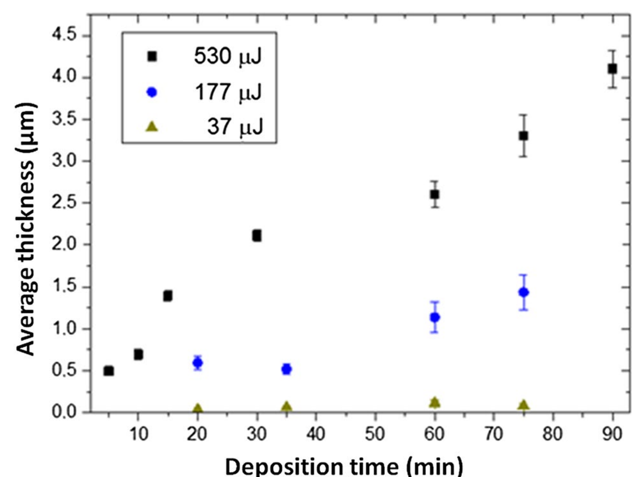

Fig. 7 Average thickness as a function of the deposition time

Fig. 7 and is shown in Fig. 8. It can be clearly seen that the growth rate has a linear dependence on the laser pulses energy (in the range used here), allowing the prediction of the deposition rate for arbitrary laser conditions.

Another worth mentioning aspect is the strong film adhesion to the substrate. Films were not easily removed by rubbing, and they did not present peeling signs, and could not be peeled off. Damage was achieved by pointy tips and the film was completely removed by repetitive scrub with textile-like materials.

The boron film morphologies were analyzed using a scanning electron microscope (TM3000 from Hitachi). A representative film (177 µJ, 60 min) micrography is shown in Fig. 9. In this micrography, it is possible to note that the film surface presents a flaky aspect.

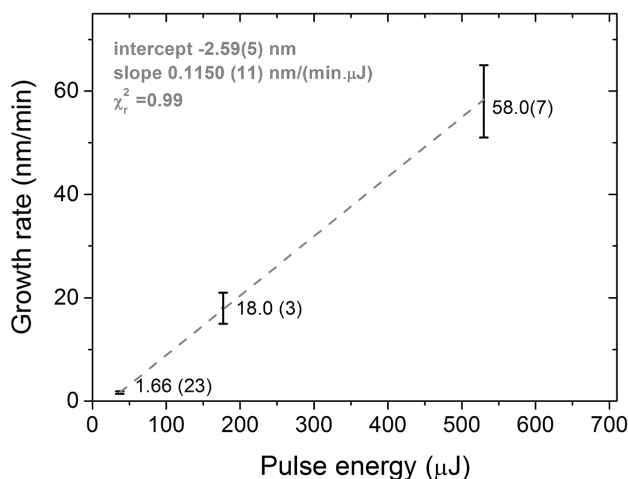

Fig. 8 Growth rate as a function of pulse energy

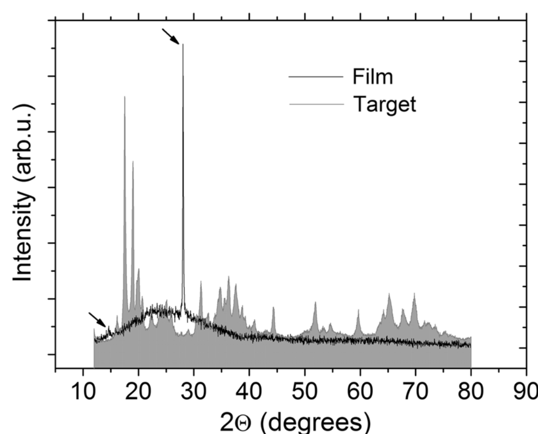

Fig. 10 X-ray diffraction analysis of the boron target (gray area) and the deposited film (black line)

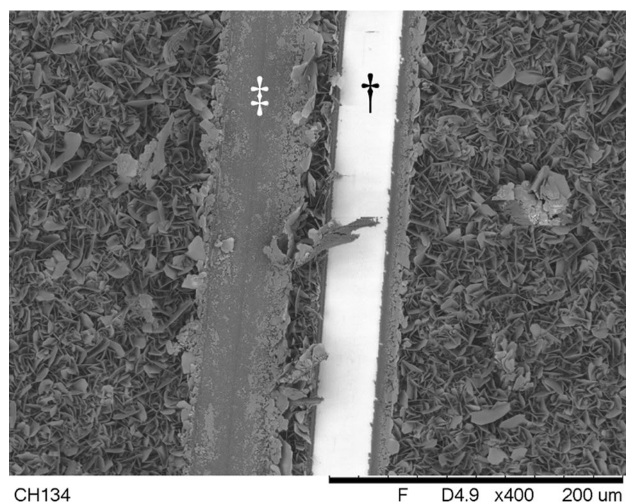

Fig. 9 SEM image of boron film 1(177 μJ, 60 min). The dagger (†) indicates the substrate (glass) revealed by the scrape, and the double dagger (‡) a superficial scratch on the film

We could not find any report on flakes being created by femtosecond PLD of metallic boron. The literature describes femtosecond PLD of boron nitrides targets, without the formation of flakes in the submicrometric scale [17]. Since the materials and SEM magnifications are different from ours, the results cannot be directly compared.

Compared with ns PLD [13, 26], our films do not present droplets, indicating that the thermal processes do not play a significant role in the ablation, as expected for fs pulses interaction with matter.

To investigate the nature of the flakes seen in Fig. 9, X-ray diffraction (XRD) measurements were done. Figure 10 shows diffractograms of the target and a 177 μJ grown film. The target exhibits a clear metallic boron crystalline structure (powder diffraction file—PDF—#80-0322), which is not reproduced in the deposited film. In the film diffractogram, the two peaks indicated by arrows show the presence of boron oxide (powder diffraction file—PDF—#13-0570), and the continuous lump denotes that the film is amorphous. The absence of common peaks suggests that there was no direct deposition of ejected boron chunks, indicating that spallation was not the main ablation mechanism.

One of the films (530 μJ, 60 min) was characterized by Ion Beam Analysis (IBA) [40] in order to verify its elemental composition. Three specific analyses were made: Rutherford backscattering spectrometry (RBS), elastic backscattering spectrometry (EBS) and nuclear reaction analysis (NRA). The combination of these three analyses results in a relation between the element concentration (% of atoms), as a function of the mass thickness (μg/cm^2), shown in Fig. 11. To better present the IBA results for the film, three different layers (boundaries) were modeled [41] to reproduce the sample structure. The film itself can be considered to occupy the first and second plateaus, the third is already a transition between film and substrate, and the fourth is the substrate. The IBA measurement uncertainties in our case are around 2%, so within this value, the first (surface) and second plateaus can be considered to have the same composition.

The presence of oxygen in boron films made by PLD has already been reported [6, 13, 26]. This oxidation can be attributed to the presence of residual water vapor and oxygen in the vacuum chamber, and also by exposure to the atmosphere. The literature reports the presence of ~20% of oxygen in Nd:YAG PLD boron films [7, 26, 42], which is compatible with our findings.

The density of the deposited films was estimated by correlating the IBA and optical profilometer results. For a 1 cm^2 deposited area, with a (2.2 ± 0.1) μm average thickness, the resulting film density is (1.74 ± 0.08) g/cm^3. The boron-only

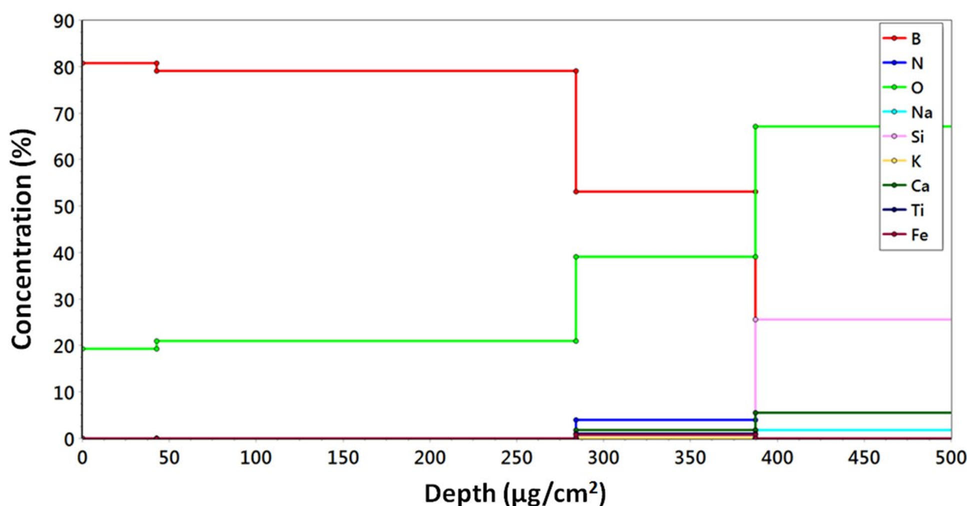

Fig. 11 Element concentration as a function of the film mass thickness (μg/cm^2) obtained by Ion Beam Analysis

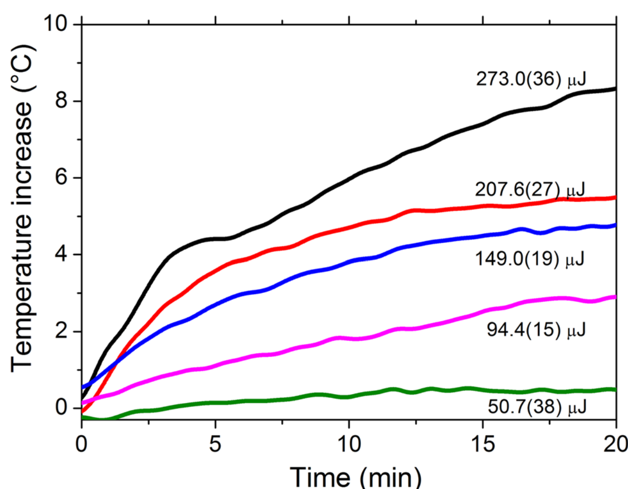

Fig. 12 Temperature behavior of 1 cm^2 glass slides under PLD

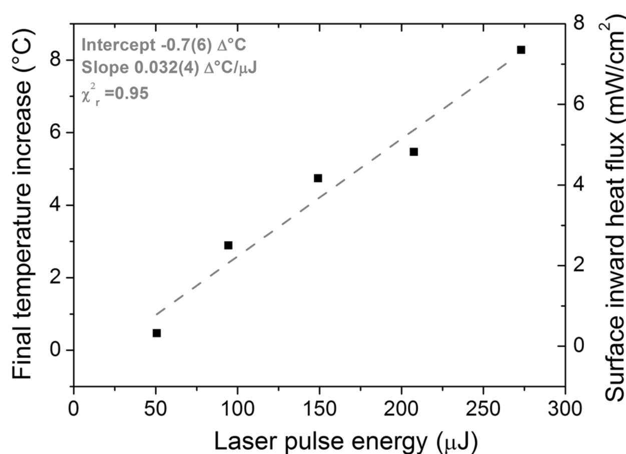

Fig. 13 Final temperature increase of 1 cm^2 glass slides

density is found by pondering its concentration (Fig. 11), which is (1.25 ± 0.06) g/cm^3, 72% of the bulk value.

As a final consideration, since one of our final goals is to deposit a boron film directly over a doped semiconductor (that will act as the α particle detector), the thermal load on the substrate is also a source of concern, because excessive heat can alter the dopant mobility, changing the semiconductor properties. To study the substrate heating, a boron PLD was done on a 150 μm-thick 1 × 1 cm^2 glass slide in the same geometry of the previous assays, with a thermocouple attached to its back with thermal paste. A 36 AWG thermocouple was used, with 140 μm diameter wires, and a very small amount of the paste was applied to minimize its thermal mass. In this evaluation, only the temperature increase was considered, and the results are shown in Fig. 12. Independently of the pulse energy, after 20 min of PLD, the substrate temperature reached a plateau, and its values are plotted in Fig. 13. Since the PLD starts with the substrate close to room temperature and the maximum temperature increase is 8 °C, no thermal effects are expected to occur in semiconductor substrates when depositing boron films under the conditions presented here.

To estimate the heat flux, a numerical model was implemented using COMSOL Multiphysics® [43]. We accounted for thermal properties, the glass surface emissivity, the mass of the thermocouple and the paste. Then the heat influx was adjusted to reproduce the slide final temperature. These results define the right-axis in Fig. 12, and can be used to calculate the final temperature of any substrate.

4 Conclusions

We have demonstrated that femtosecond PLD is a viable way to produce thick boron films to be used as neutron converters. The produced films show a good adhesion to the substrate, do

not peel off and present a low concentration of contaminants (oxygen), with a density close to the bulk.

The film thickness was observed to grow linearly with the laser energy and deposition time, allowing the design of the conditions to produce an arbitrary film.

A methodology to estimate the films thicknesses was presented. We think that this is important for PLD, since films deposited over large areas (a few cm^2) present a variable thickness, and this is not usually discussed in the literature.

The morphological analyses revealed the absence of droplets in the films, and the DRX results have shown that they lack any crystalline structure, as observed in the target, indicating that spallation is not a major ablation mechanism (under the conditions used un this work). The amorphous film structure revealed by the DRX does not an impeditive neutron conversion.

The SEM micrographies have shown that the films have a flaky structure, pointing out that their densities are lower than that of the metallic crystalline lattice, which is confirmed by the density calculated from the IBA and profilometer analysis.

We could not determine the mechanism that created the flakes, but we can rule out two possibilities: they are not a spallation product or a polycrystalline growth. If any of those mechanisms played a major part, a crystalline structure would appear on the films' X-ray diffractograms. Notwithstanding, these structures do not interfere with the aimed application and should be a subject for future research.

Finally, the heat flux from the PLD process is small, showing that this femtosecond technique can be used in a variety of substrates, including temperature sensitive materials such as polymers.

Acknowledgements We would like to thank the National Council for Scientific and Technological Development (CNPq): projects 465763/2014-6 and 141628/2015-4; Secretary of Strategic Affairs; Lamfi (Laboratory of material analyses using ion beams—São Paulo University); the support given by the Center for Lasers and Applications' Multiuser Facility at IPEN-CNEN/SP and the Nuclear Fuel Center Multiuser Facility X-Ray Diffraction Laboratory at IPEN-CNEN/SP.

Data Availability The raw/processed data required to reproduce these findings cannot be shared at this time as the data also form part of an ongoing study, but are available from the corresponding author on reasonable request.

Compliance with ethical standards

Conflict of interest The authors declare that they have no conflict of interest.

References

1. C.C. Klepper, R.C. Hazelton, E.J. Yadlowsky, E.P. Carlson, M.D. Keitz, J.M. Williams, R.A. Zuhr, D.B. Poker, J. Vac. Sci. Technol. A Vac. Surf. Film **20**, 725 (2002)
2. C.C. Klepper, J.M. Williams, J.J. Truhan, J. Qu, L. Riester, R.C. Hazelton, J.J. Moschella, P.J. Blau, J.P. Anderson, O.O. Popoola, M.D. Keitz, Thin Solid Films **516**, 3070 (2008)
3. M. Vidal-Dasilva, M. Fernández-Perea, J.A. Méndez, J.A. Aznárez, J.I. Larruquert, Appl. Opt. **47**, 2926 (2008)
4. S. Roszeitis, B. Feng, H.P. Martin, A. Michaelis, J. Eur. Ceram. Soc. **34**, 327 (2014)
5. J.E. Martin, *Physics for Radiation Protection, Third Edition* (2013)
6. P. Costa, M.P. Raele, R.E. Samad, N.D. Vieira, N.G.P. Machado, F.A. Genezini, in *High-Power Laser Mater Process Appl Diagnostics, Syst VII*, ed. by S. Kaierle, S.W. Heinemann (SPIE, Bellingham, 2018), p. 18
7. Z.F. Song, S.Z. Ye, Z.Y. Chen, L. Song, J. Shen, Appl. Radiat. Isot. **69**, 443 (2011)
8. D.S. McGregor, R.T. Klann, H.K. Gersch, J.D. Sanders, IEEE Nucl. Sci. Symp. Med. Imaging Conf. **4**, 2454 (2002)
9. P. Costa, M.P. Raele, H. Yoriyaz, P. de T.D. Siqueira, G.S. Zahn, F.A. Genezini, in *Ina 2015 Int Nucl Atl Conf Brazilian Nucl Progr State Policy a Sustain World* (Brazil, 2015)
10. C. Höglund, J. Birch, K. Andersen, T. Bigault, J.-C. Buffet, J. Correa, P. van Esch, B. Guerard, R. Hall-Wilton, J. Jensen, A. Khaplanov, F. Piscitelli, C. Vettier, W. Vollenberg, L. Hultman, J. Appl. Phys. **111**, 104908 (2012)
11. Z. Wang, C.L. Morris, Nucl. Instrum. Methods Phys. Res. Sect. A Accel. Spectrom. Detect. Assoc. Equip. **651**, 323–325 (2011)
12. K.A. Nelson, N.S. Edwards, N.J. Hinson, C.D. Wayant, D.S. McGregor, Nucl. Instrum. Methods Phys. Res. Sect. A Accel. Spectrom. Detect. Assoc. Equip. **767**, 14 (2014)
13. Z. Wang, Y. Shimizu, T. Sasaki, K. Kirihara, K. Kawaguchi, K. Kimura, N. Koshizaki, J. Solid State Chem. **177**, 1639 (2004)
14. G. Celentano, A. Vannozzi, A. Mancini, A. Santoni, A. Pietropaolo, G. Claps, E. Bemporad, M. Renzelli, F. Murtas, L. Quintieri, Surf. Coat. Technol. **265**, 160 (2015)
15. P. Chaudhari, A. Singh, A. Topkar, R. Dusane, Nucl. Instrum. Methods Phys. Res. Sect. A Accel. Spectrom. Detect. Assoc. Equip. **779**, 33 (2015)
16. R.J. Nikolić, A.M. Conway, C.E. Reinhardt, R.T. Graff, T.F. Wang, N. Deo, C.L. Cheung, Appl. Phys. Lett. **93**, 133502 (2008)
17. T. Shimizu, T. Nakamura, S. Sato, in edited by V.I. Vlad (2007), p. 67850E–67850E–8
18. N. Acacia, E. Fazio, F. Neri, P.M. Ossi, S. Trusso, N. Santo, Radiat. Eff. Defects Solids **163**, 293 (2008)
19. P.R. Willmott, J.R. Huber, Rev. Mod. Phys. **72**, 315 (2000)
20. P. Kelly, R. Arnell, Vacuum **56**, 159 (2000)
21. D. Benetti, R. Nouar, R. Nechache, H. Pepin, A. Sarkissian, F. Rosei, J.M. MacLeod, Sci. Rep. **7**, 2503 (2017)
22. E.-S. Lee, J.-K. Park, W.-S. Lee, T.-Y. Seong, Y.-J. Baik, Methods Mater. Int. **19**, 1323 (2013)
23. S.I. Anisimov, D. Bäuerle, B.S. Luk'yanchuk, Phys. Rev. B **48**, 12076 (1993)
24. F. Kokai, M. Taniwaki, K. Takahashi, A. Goto, M. Ishihara, K. Yamamoto, Y. Koga, Diam. Relat. Mater. **10**, 1412 (2001)
25. Z. Wang, Y. Shimizu, T. Sasaki, K. Kawaguchi, K. Kimura, N. Koshizaki, Chem. Phys. Lett. **368**, 663 (2003)
26. D. Dellasega, V. Russo, A. Pezzoli, C. Conti, N. Lecis, E. Besozzi, M. Beghi, C.E. Bottani, M. Passoni, Mater. Des. **134**, 35 (2017)
27. K.-H. Leitz, B. Redlingshöfer, Y. Reg, A. Otto, M. Schmidt, Phys. Procedia **12**, 230 (2011)

28. C.W. Schneider, T. Lippert, in *Laser Process Mater Fundam Appl Dev*, ed. by P. Schaaf (Springer, Berlin, 2010), pp. 89–112
29. D. von der Linde, K. Sokolowski-Tinten, Appl. Surf. Sci. **154**, 1 (2000)
30. N.M. Bulgakova, A.V. Bulgakov, V.P. Zhukov, W. Marine, A.Y. Vorobyev, C. Guo, in *Proc SPIE 7005, High-Power Laser Ablation VII*, edited by C.R. Phipps (2008), p. 70050C
31. B.N. Chichkov, C. Momma, S. Nolte, F. Alvensleben, A. Tünnermann, Appl. Phys. A Mater. Sci. Process. **63**, 109 (1996)
32. N.M. Bulgakova, I.M. Bourakov, Appl. Surf. Sci. **197–198**, 41 (2002)
33. P. Lorazo, L.J. Lewis, M. Meunier, Phys. Rev. Lett. **91**, 225502 (2003)
34. L.V. Zhigilei, Z. Lin, D.S. Ivanov, J. Phys. Chem. C **113**, 11892 (2009)
35. S.I. Kudryashov, A.A. Ionin, S.V. Makarov, N.N. Mel'nik, L.V. Seleznev, D.V. Sinitsyn, in *AIP Conference Proceedings* (2012), pp. 244–255
36. E.G. Gamaly, A.V. Rode, B. Luther-Davies, V.T. Tikhonchuk, Phys. Plasmas **9**, 949 (2002)
37. A. Sikora, A. Berkesse, O. Bourgeois, J.-L. Garden, C. Guerret-Piécourt, A.-S. Loir, F. Garrelie, C. Donnet, Appl. Phys. A **94**, 105 (2009)
38. L.M. Machado, R.E. Samad, W. de Rossi, N.D.V. Junior, Opt. Express. **20**, 4114 (2012)
39. Y. Jee, M.F. Becker, R.M. Walser, J. Opt. Soc. Am. B **5**, 648 (1988)
40. M.H. Tabacniks, *The Laboratory for Material Analysis with Ion Beams LAMFI-USP* (World Scientific, Singapore, 1997)
41. T.F. Silva, C.L. Rodrigues, M. Mayer, M.V. Moro, G.F. Trindade, F.R. Aguirre, N. Added, M.A. Rizzutto, M.H. Tabacniks, Nucl. Instrum. Methods Phys. Res. Sect. B Beam Interact. Mater. Atoms. (2016)
42. D. Mijatovic, A. Brinkman, H. Hilgenkamp, H. Rogalla, G. Rijnders, D.H.A. Blank, Appl. Phys. A **79**, 1243 (2004)
43. COMSOL Multiphysics, *Manual* (2009)